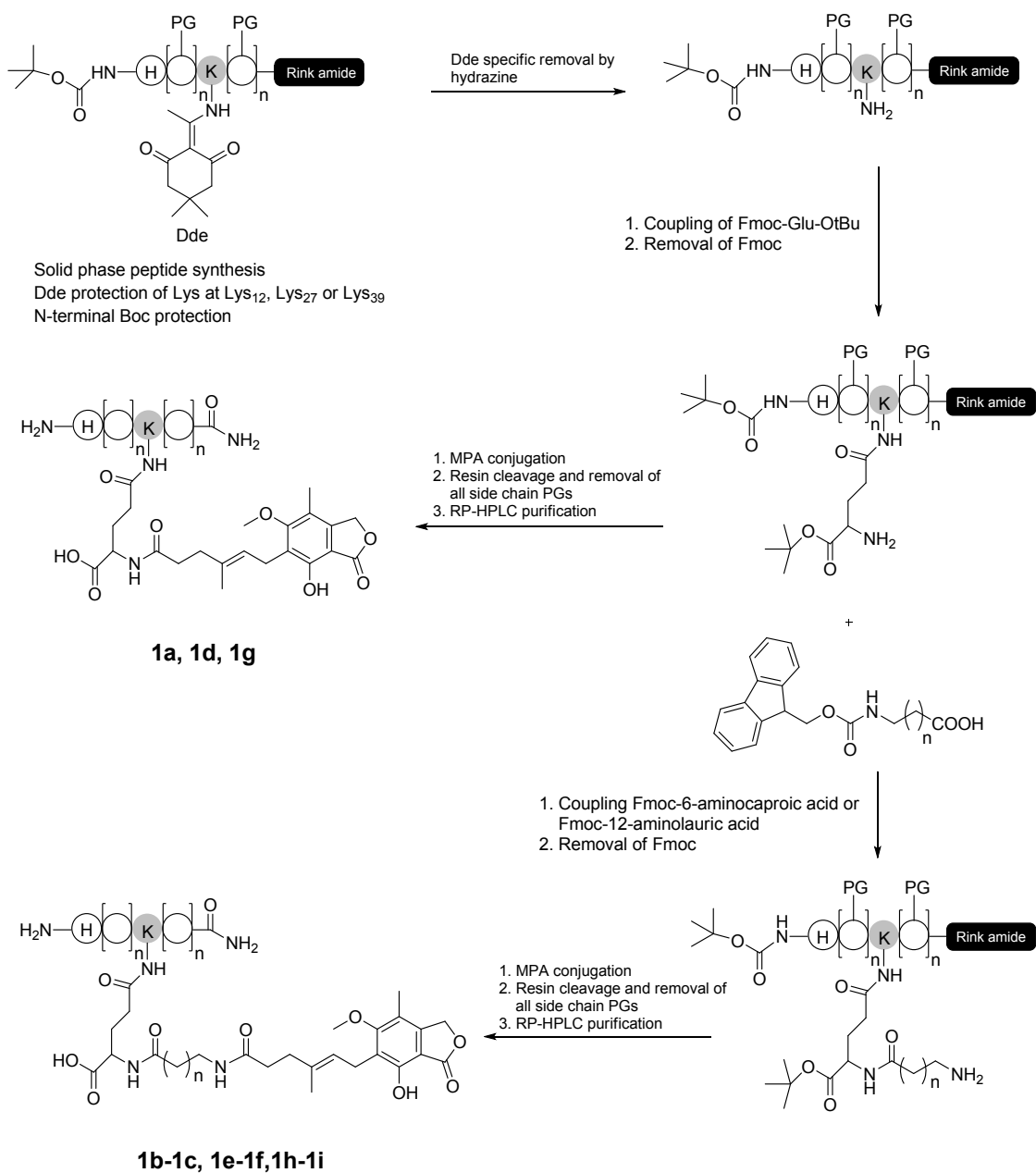


Discovery of Lixisenatide Analogue as Long-acting Hypoglycemic Agents Using Novel Peptide Half-Life Extension Technology Based on Mycophenolic Acid

Chunli Tang[#], Qing Li[#], Xiaoyan Deng, Weiwei Wu, Liufeng Liao, Kai Liang, Rongrui Huo,
Chenglin Li, Jing Han^{*}, Weizhong Tang^{*}, Neng Jiang^{*}

Synthetic route of 1a–1i (Scheme S1)	S2
Characterization of 1a–1i	S3-S7
Synthetic route of 2a (Scheme S2)	S8
Synthetic route of 2b–2d (Scheme S3)	S9
Characterization of 2a–2d	S10-S11
The studies of the impurity profile of 2c and the impact of the impurity in 2c on the biological activity of 2c	S12-S16
<i>In vivo</i> toxicity of the impurity in 2c	S17



Scheme S1. Synthetic route of **1a–1i**. PG: Acid labile protecting group.

HPLC conditions for all compounds (Agilent technologies 1260 infinity)

Column: Shim-pack PREP-ODS(H) KIT (5 μm , 250 mm \times 4.6 mm);

Mobile phase: mobile phase A: water with 0.1% TFA, mobile phase B: methanol;

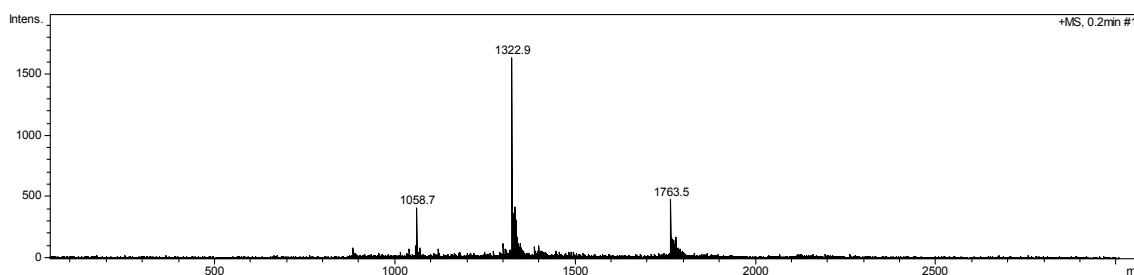
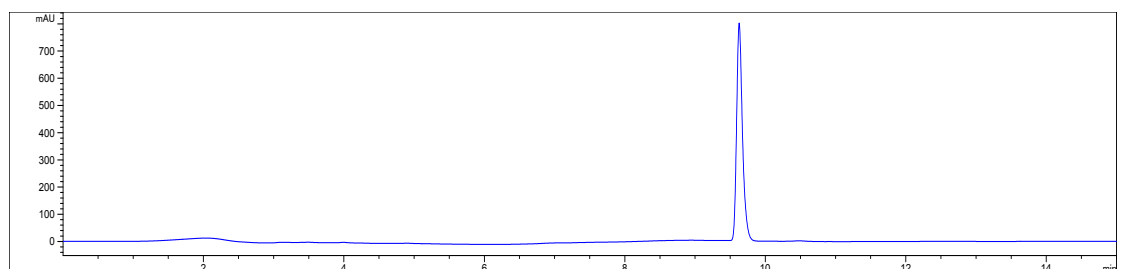
0-7 min, 30-90% B; 7-13 min, 90-90% B; 13-14 min, 90-50% B; 14-15 min, 50-50% B;

Wavelength: 214 nm;

Rate: 0.8 mL/min;

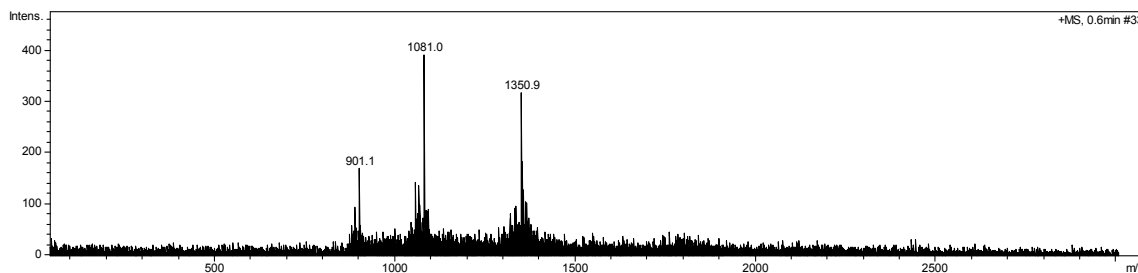
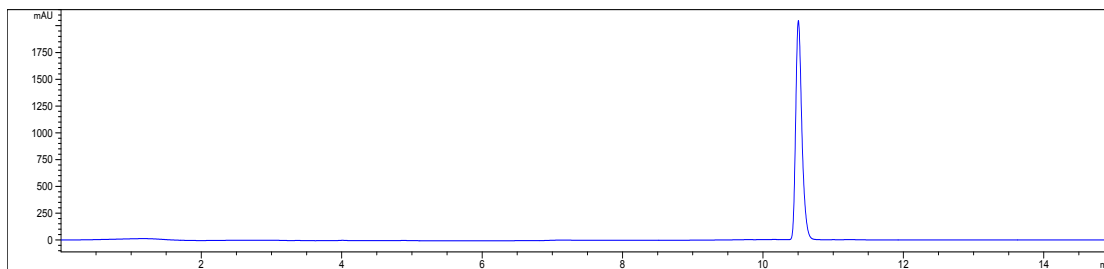
Temperature: 25 $^{\circ}\text{C}$.

1a



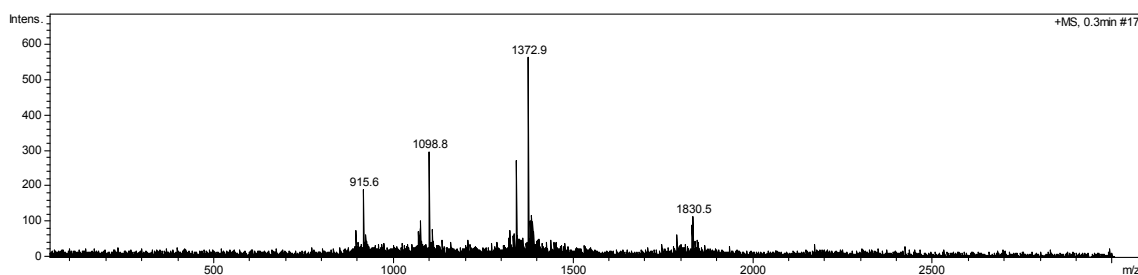
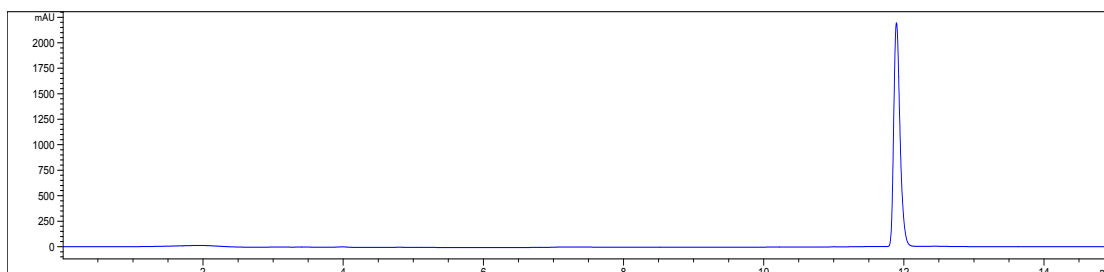
(m/z)calad	(m/z)found
$[\text{m}+3\text{H}]^{3+}$ 1764.3	$[\text{m}+3\text{H}]^{3+}$ 1763.5
$[\text{m}+4\text{H}]^{4+}$ 1323.5	$[\text{m}+4\text{H}]^{4+}$ 1322.9

1b



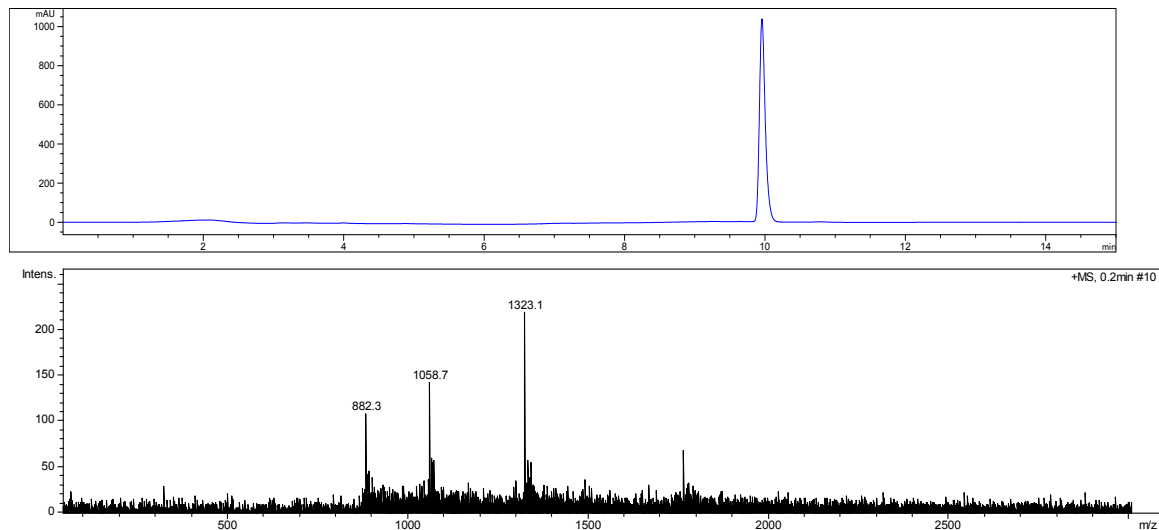
(m/z)calad	(m/z)found
$[m+4H]^{4+}$ 1351.8	$[m+4H]^{4+}$ 1350.9
$[m+5H]^{5+}$ 1081.6	$[m+5H]^{5+}$ 1081.0

1c



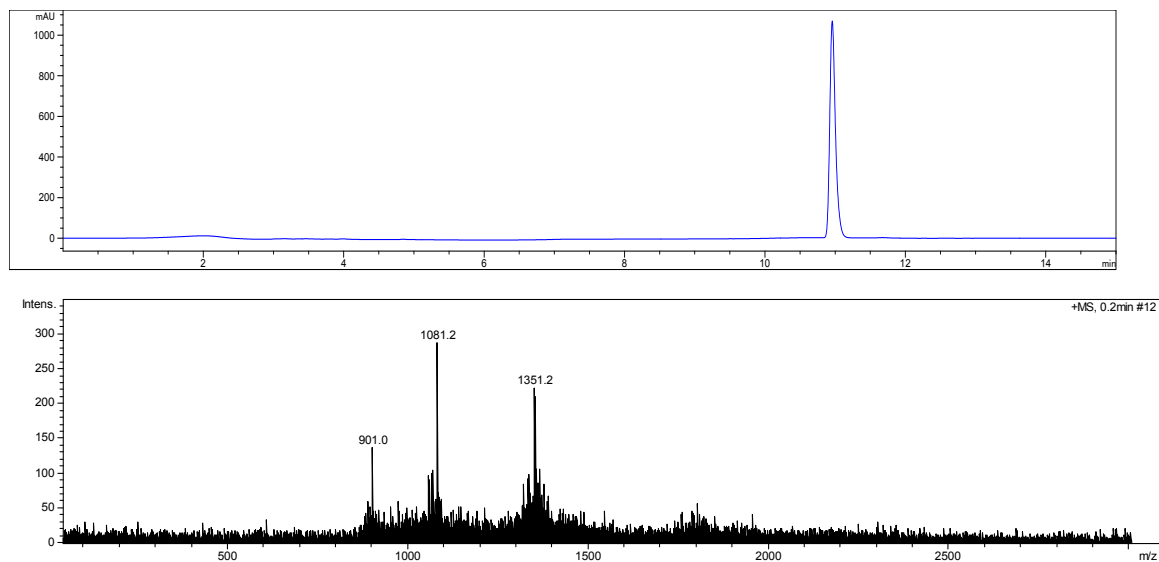
(m/z)calad	(m/z)found
$[m+3H]^{3+}$ 1830.1	$[m+3H]^{3+}$ 1830.5
$[m+4H]^{4+}$ 1372.8	$[m+4H]^{4+}$ 1372.9

1d



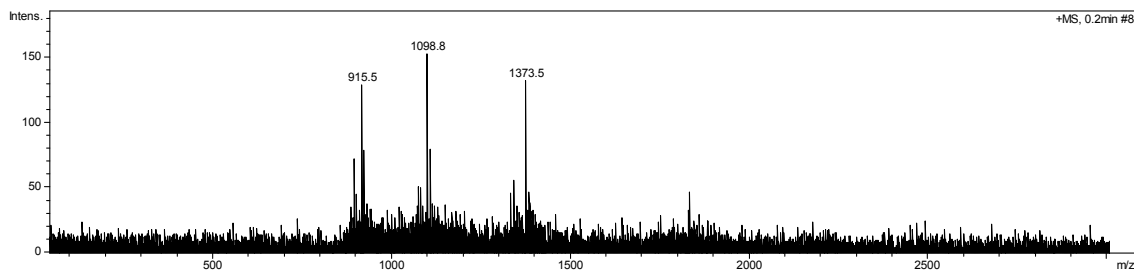
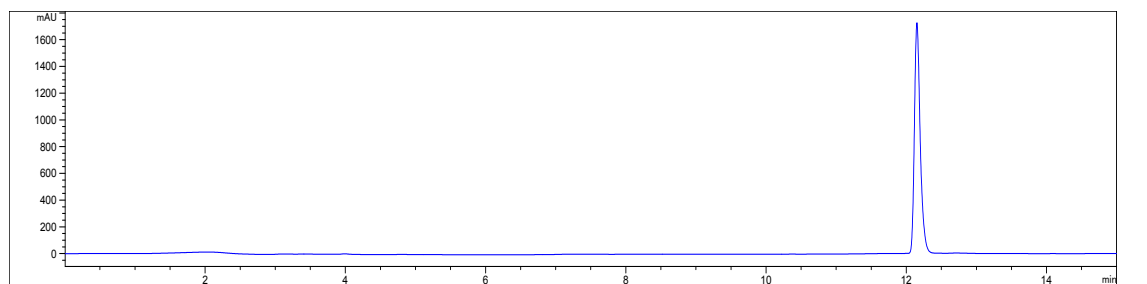
(m/z)calad	(m/z)found
[m+4H] ⁴⁺ 1323.5	[m+4H] ⁴⁺ 1323.1
[m+5H] ⁵⁺ 1059.0	[m+5H] ⁵⁺ 1058.7

1e



(m/z)calad	(m/z)found
[m+4H] ⁴⁺ 1351.8	[m+4H] ⁴⁺ 1351.2
[m+5H] ⁵⁺ 1081.6	[m+5H] ⁵⁺ 1081.2

1f



(m/z)calad

(m/z)found

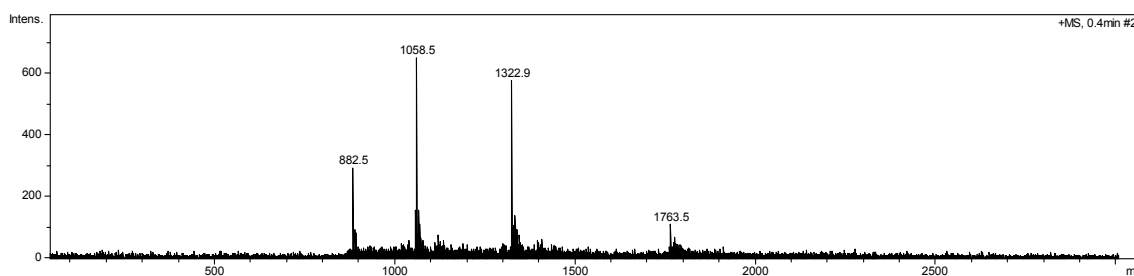
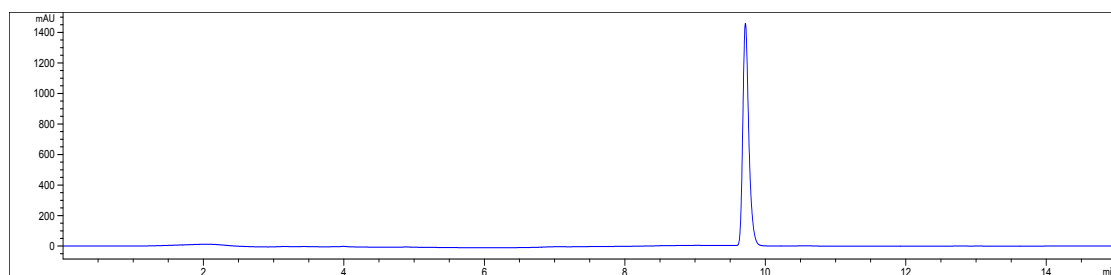
[m+4H]⁴⁺ 1372.8

[m+4H]⁴⁺ 1373.5

[m+5H]⁵⁺ 1098.4

[m+5H]⁵⁺ 1098.8

1g



(m/z)calad

(m/z)found

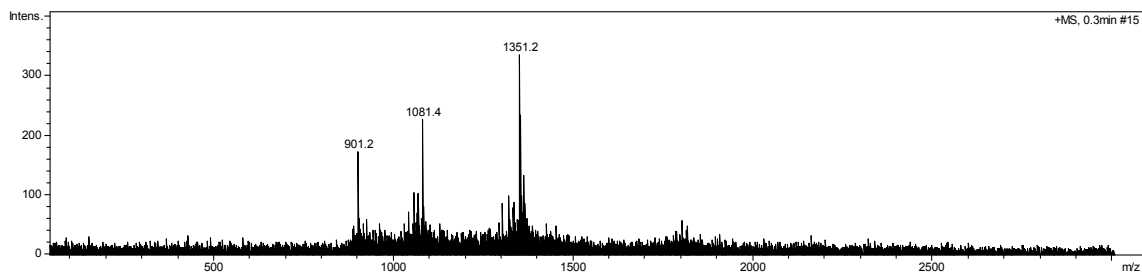
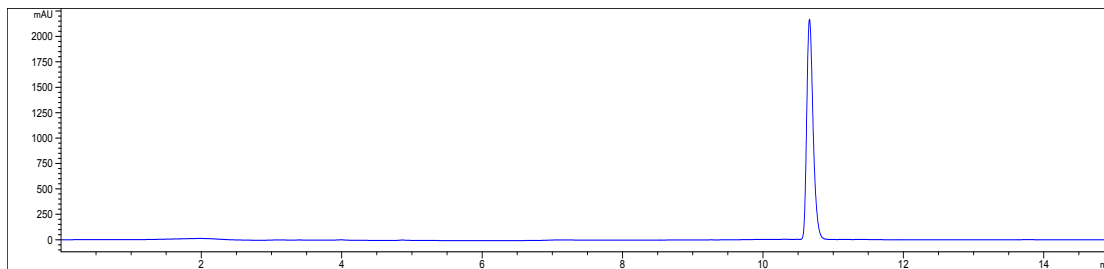
[m+4H]⁴⁺ 1323.5

[m+4H]⁴⁺ 1323.1

[m+5H]⁵⁺ 1059.0

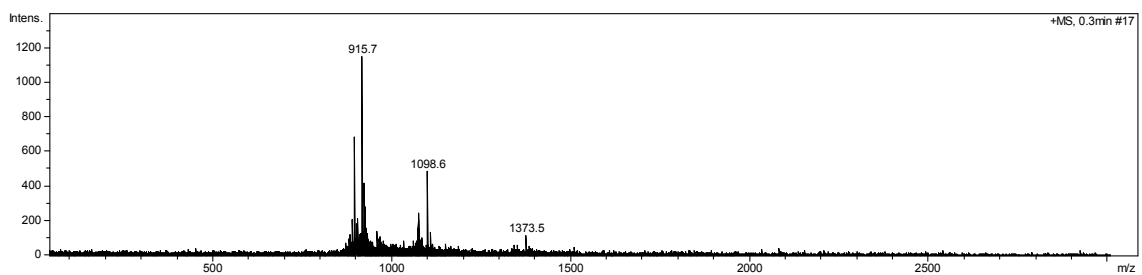
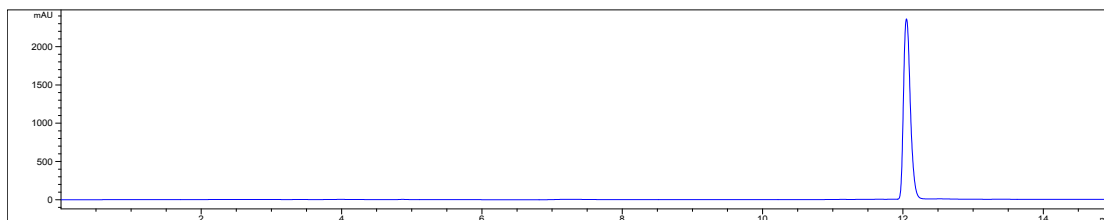
[m+5H]⁵⁺ 1058.7

1h

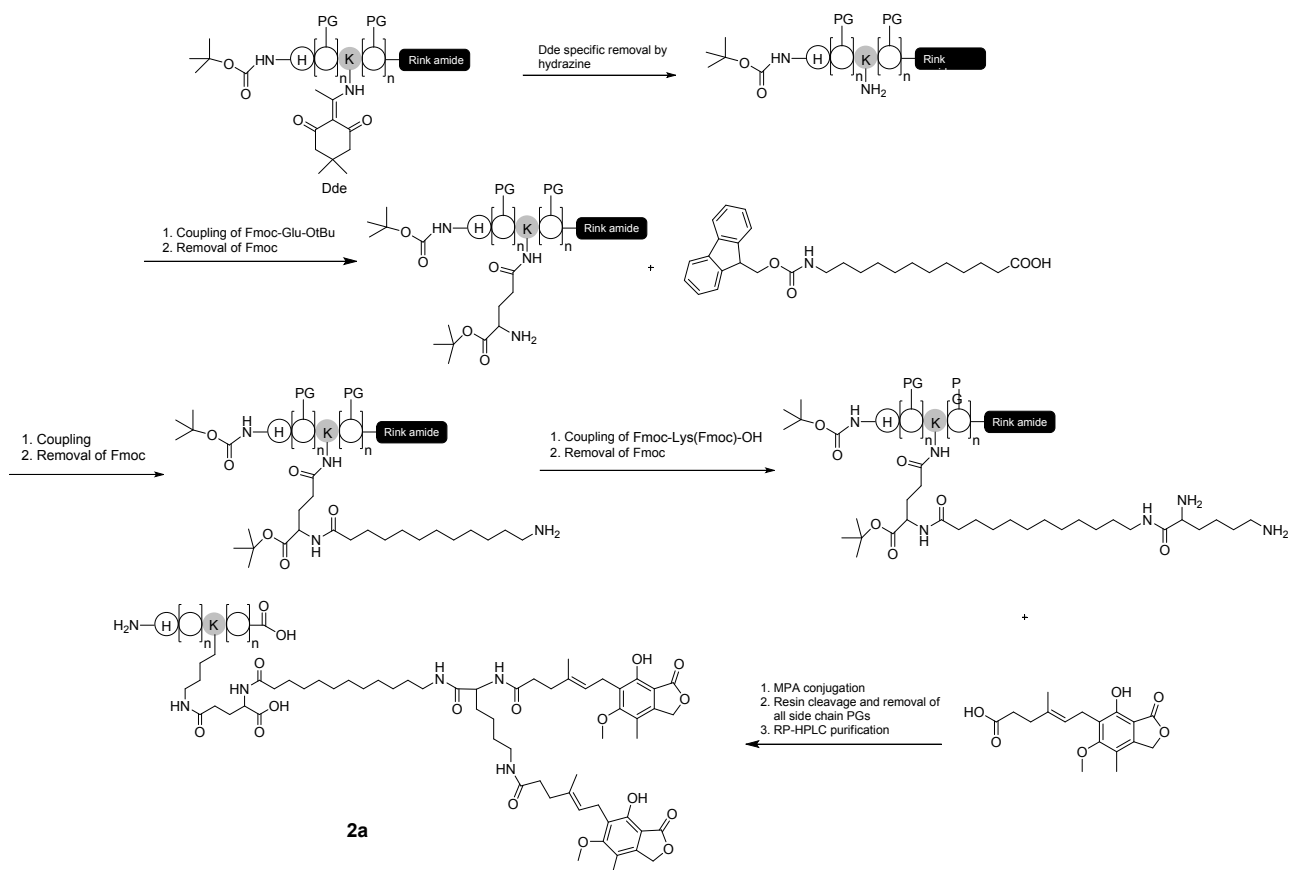


(m/z)calad	(m/z)found
$[m+4H]^{4+}$ 1351.8	$[m+4H]^{4+}$ 1351.2
$[m+5H]^{5+}$ 1081.6	$[m+5H]^{5+}$ 1081.2

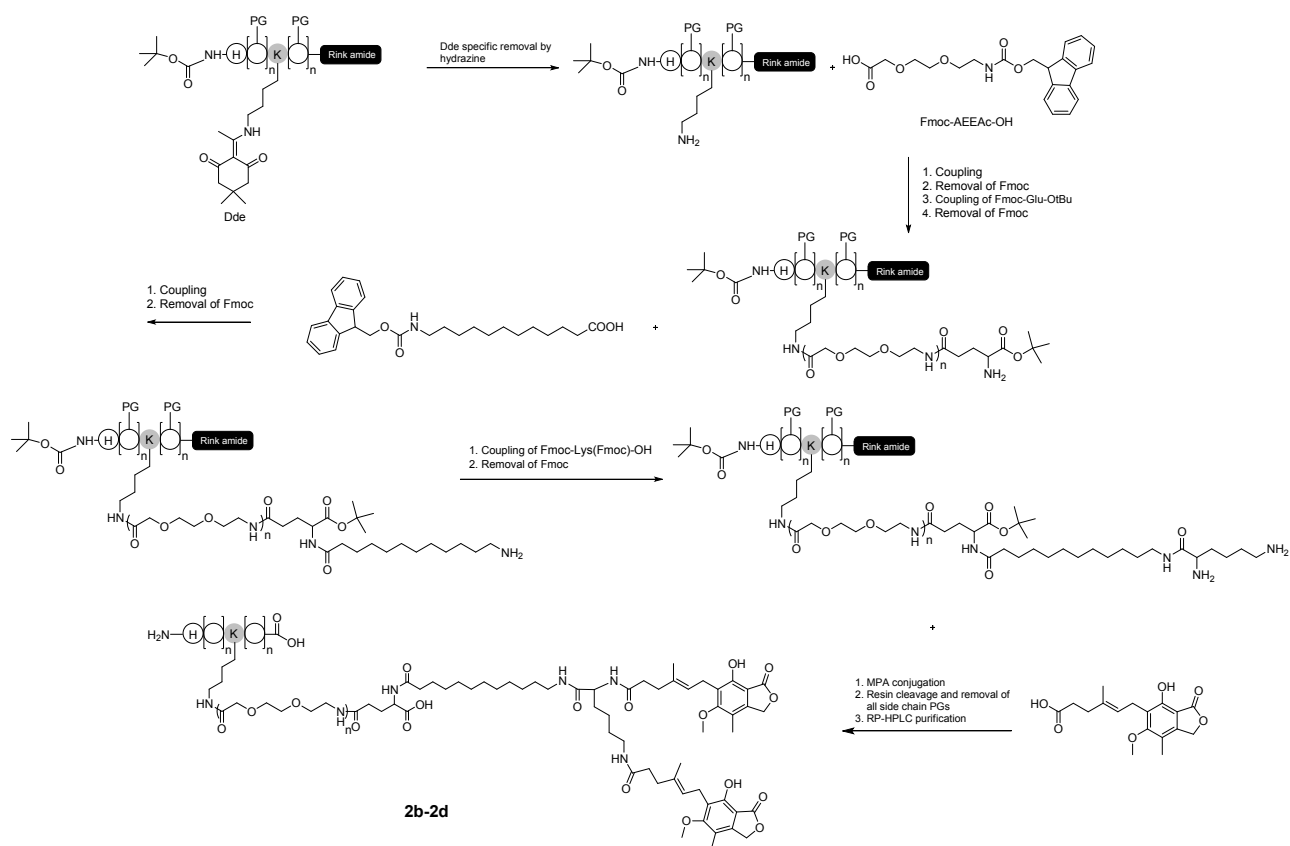
1i



(m/z)calad	(m/z)found
$[m+5H]^{5+}$ 1098.4	$[m+5H]^{5+}$ 1098.6
$[m+6H]^{6+}$ 915.6	$[m+6H]^{6+}$ 915.7

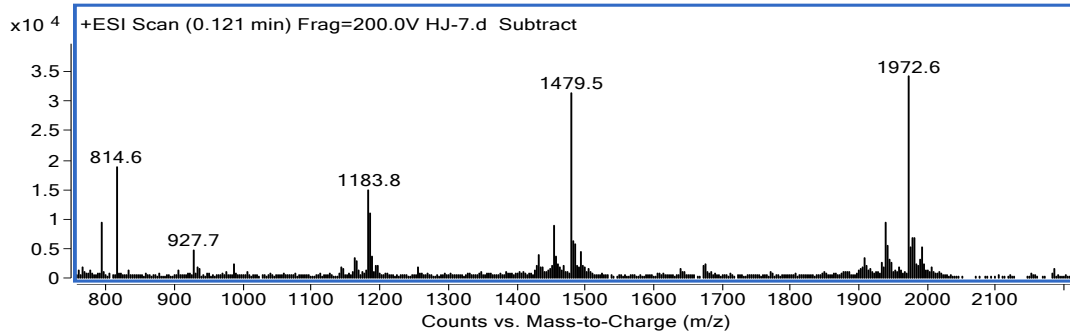
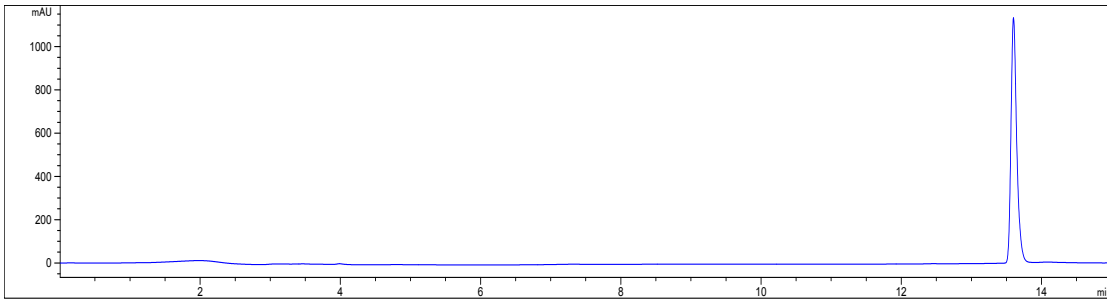


Scheme S2. Synthetic route of **2a**. PG: Acid labile protecting group.



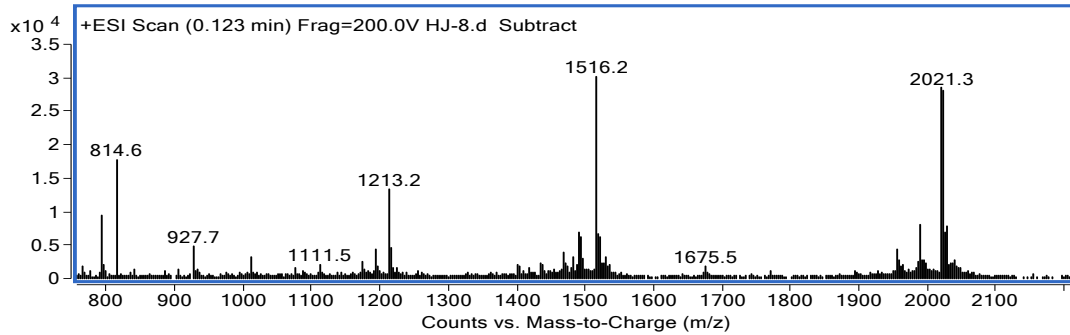
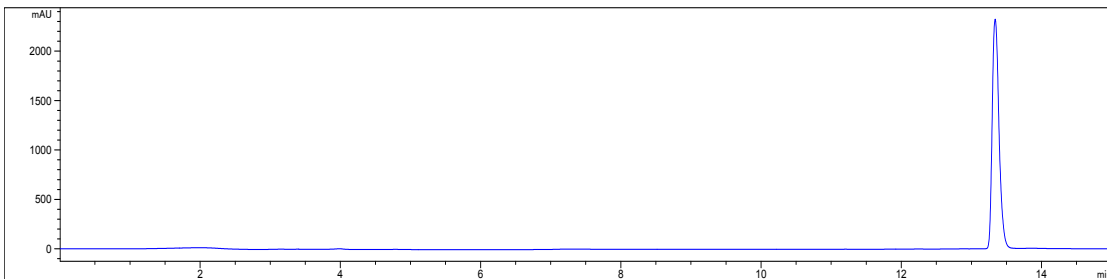
Scheme S3. Synthetic route of **2b–2d**. PG: Acid labile protecting group

2a



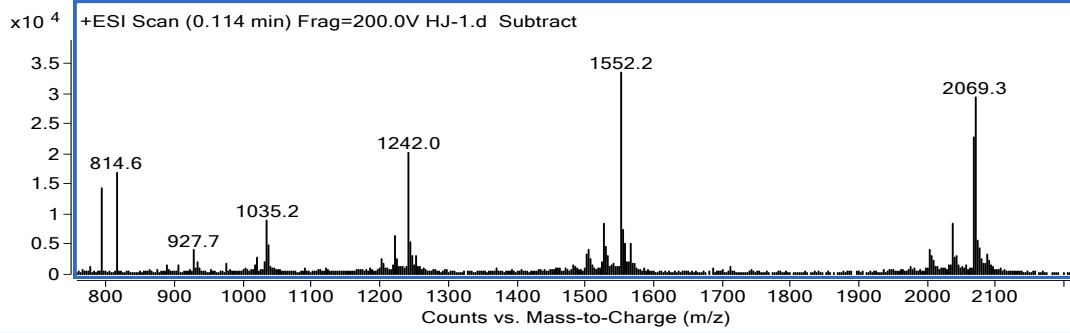
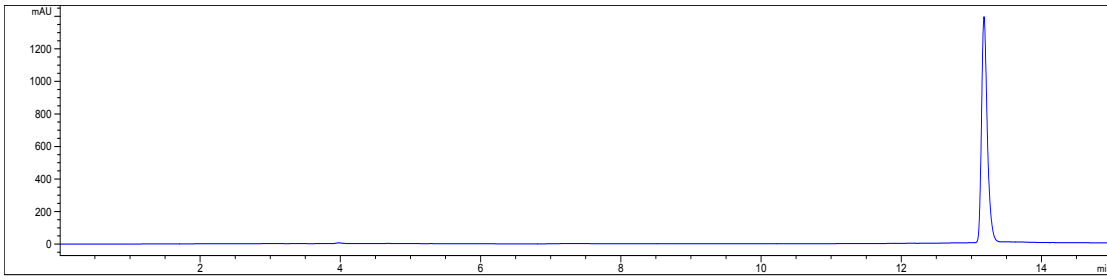
(m/z)calad	(m/z)found
$[m+4H]^{4+}$ 1480.5	$[m+4H]^{4+}$ 1479.5
$[m+5H]^{5+}$ 1184.6	$[m+5H]^{5+}$ 1183.8

2b



(m/z)calad	(m/z)found
$[m+4H]^{4+}$ 1516.8	$[m+4H]^{4+}$ 1516.2
$[m+5H]^{5+}$ 1213.6	$[m+5H]^{5+}$ 1213.2

2c



(m/z)calad

(m/z)found

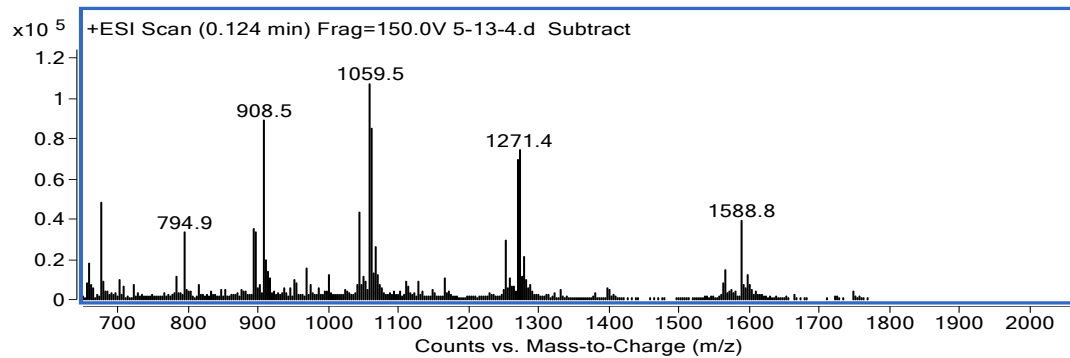
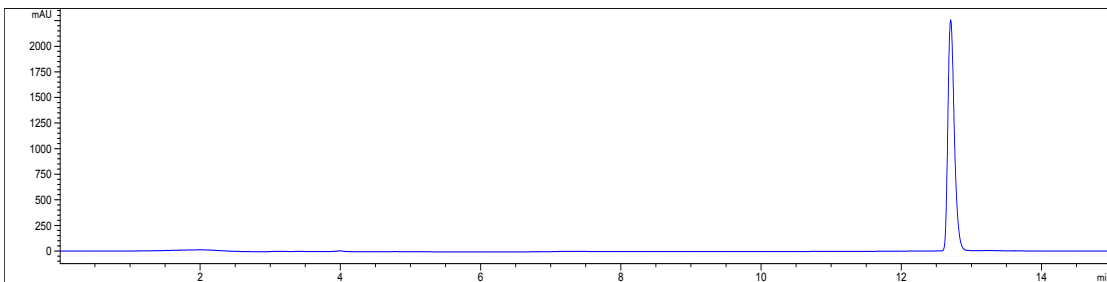
[m+4H]⁴⁺ 1553.0

[m+4H]⁴⁺ 1552.2

[m+5H]⁵⁺ 1242.6

[m+5H]⁵⁺ 1242.0

2d



(m/z)calad

(m/z)found

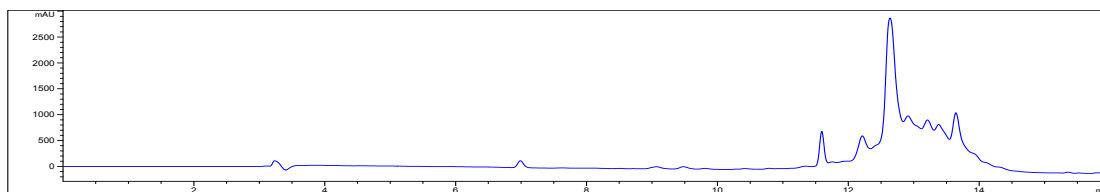
[m+4H]⁴⁺ 1589.3

[m+4H]⁴⁺ 1588.8

[m+5H]⁵⁺ 1271.7

[m+5H]⁵⁺ 1271.4

The studies of the impurity profile of **2c** and the impact of the impurity in **2c** on the biological activity of **2c**.



The HPLC spectrum of crude **2c**.

HPLC conditions (Agilent technologies 1260 infinity):

Column: Thermo C18 reversed-phase column (5 μm , 150 mm \times 4.6 mm);

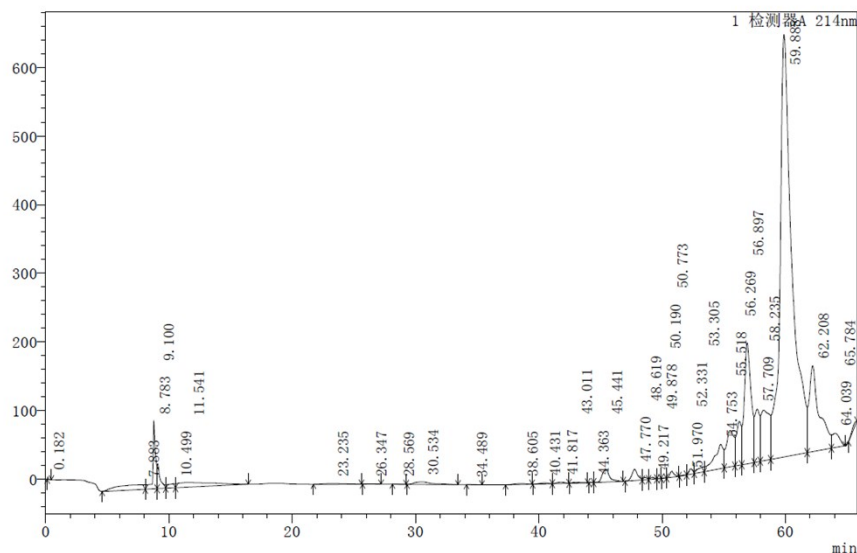
Mobile phase: mobile phase A: water with 0.1% TFA, mobile phase B: methanol;

Method: 0-7 min, 30-90% B; 7-13 min, 90-90% B; 13-14 min, 90-50% B; 14-16 min, 50-50% B;

Wavelength: 214 nm;

Rate: 1 mL/min;

Temperature: 25°C.



Representative spectrum during the purification of **2c** using RP-HPLC.

HPLC conditions (Shimadzu LC-20AP):

Column: Thermo Hypersil GOLD C18 reversed-phase column (12 μm , 250 \times 20 mm);

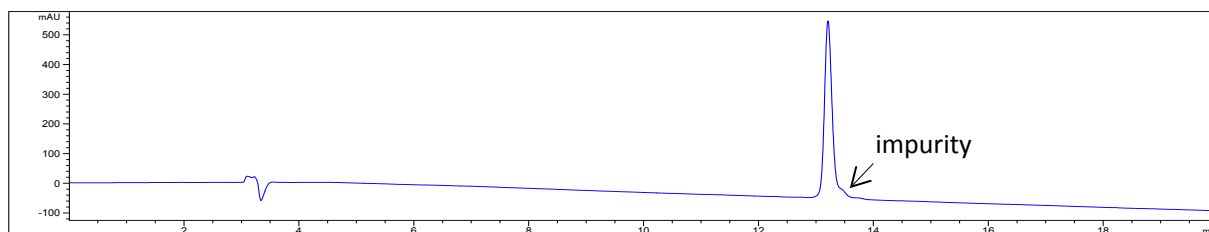
Mobile phase: mobile phase A: water with 0.1% TFA, mobile phase B: methanol;

Method: 0-5 min, 40-40% B; 5-40 min, 40-85% B; 40-80 min, 85-85% B;

Wavelength: 214 nm;

Rate: 7 mL/min;
Temperature: 25°C.

After purification and freeze drying, the purified **2c** was dissolved and the purity of **2c** was re-analyzed.



The spectrum of **2c** after first purification.

HPLC conditions (Agilent technologies 1260 infinity):

Column: Shim-pack PREP-ODS(H) KIT (5 μ m, 250 mm \times 4.6 mm);

Mobile phase: mobile phase A: water with 0.1% TFA, mobile phase B: methanol;

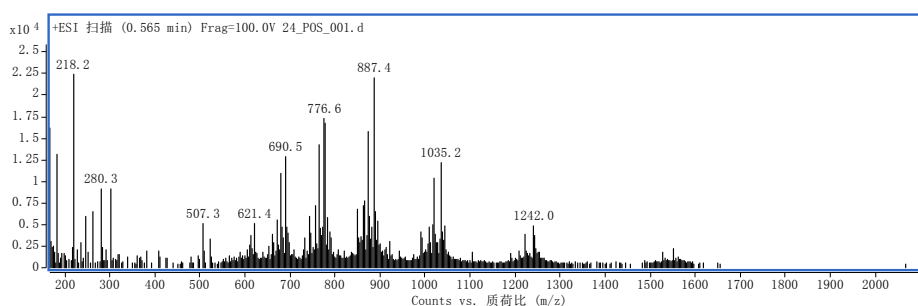
Method: 0-7 min, 30-90% B; 7-13 min, 90-90% B; 13-14 min, 90-50% B; 14-20 min, 50-50% B;

Wavelength: 214 nm;

Rate: 0.8 mL/min;

Temperature: 25°C.

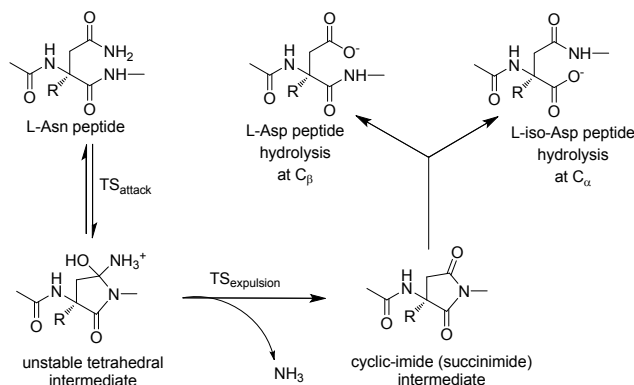
The HPLC trace indicated impurity at the right tail of the peak of **2c**. The impurity was speared and analyzed by MS.



The MS spectrum of the impurity in **2c**.

We noticed that the MS spectrum of the impurity was very similar to **2c**, and we assume it as the deamidation byproduct at Asn₂₈. Compared with **2c** (MW = 6208.1), the MW of deamidation product is 6209.1, and this explains the similarity of the MS spectra between **2c** and the impurity.

Deamidation can occur in aqueous media, particularly under basic conditions, leading to the formation of α - and β -aspartyl peptides. It is most problematic with peptides containing Asn-Gly and Asn-Ser. We speculate that the deamidation product is easily formed due to the Asn₂₈-Gly₂₉ residues in the sequence of **2c**.



The mechanism of the Asn deamidation reaction at neutral and basic pH.

After a second purification, we successfully obtained **2c** with a purity >99%, which was used in our original biological activity studies. We further compared the *in vivo* hypoglycemic, insulinotropic, and glucose-stabilizing activities of **2c** after first purification (referred to as impur-**2c**) and second purification (referred to as **2c**).

Methods

Glucoregulatory and insulinotropic assay

The effects of impur-**2c** and **2c** on glucoregulatory and insulinotropic were tested by IPGTT on *db/db* mice. Mice (n = 6) were fasted overnight (16 h) and then *i.p.* injected with saline (control), impur-**2c** and **2c** (25 nmol·kg⁻¹) 30 min prior to the glucose load. The glucose (1 g·kg⁻¹) was *i.p.* loaded at 0 min. Tail vein blood was drawn for blood glucose levels measurement at -30 and 0, 10, 15, 30, 45, 60, and 120 min by using one-touch glucometer, and for plasma insulin measurement at 0, 15, 30, and 60 min by using mouse insulin ELISA kit (Nanjing Jiancheng Bioengineering Institute, Jiangsu, China).

Glucose-stabilizing activity in db/db mice

The hypoglycemic activities of impur-**2c** and **2c** were measured in *db/db* mice (n = 6) under non-fasted condition. The mice were allowed to free access to food. On the experiment day, mice were

s.c. injected with saline (control), impur-**2c** and **2c** (25 nmol·kg⁻¹) at t = 0 h. The blood was obtained and the blood glucose levels were measured using the same method described above at 0, 4, 6, 12, 24 and 48 h.

Results

As shown in Figure S1, the *in vivo* hypoglycemic, insulinotropic and glucose-stabilizing activities between impur-**2c** and **2c** are very similar, indicating that the minimal amount of impurity in **2c** did not cause serious biological activities lost.

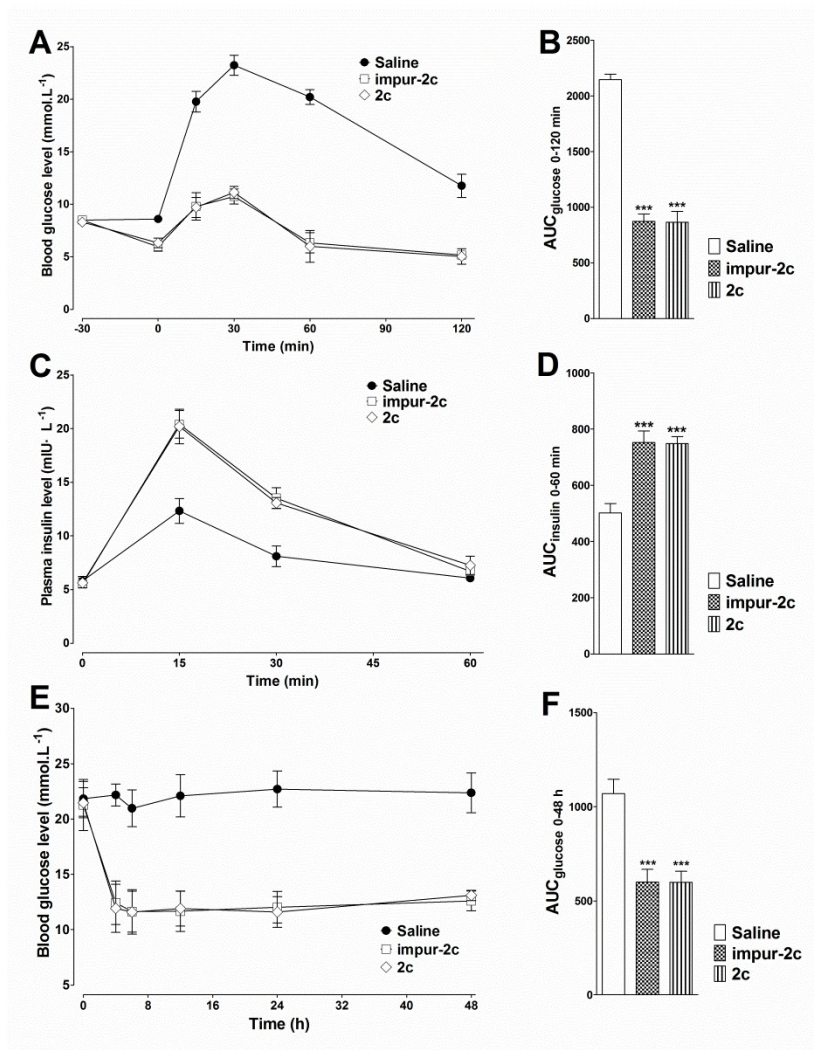


Figure S1. Glucose-lowering and insulinotropic activities of impur-**2c** and **2c** were determined by IPGTT in *db/db* mice. The time-response curves of blood glucose (A) and plasma insulin concentrations (C). The calculated AUC values of blood glucose (B) and plasma insulin (D). Glucose-stabilizing activities of impur-**2c** and **2c** were determined in non-fasted *db/db* mice. The

time-response curves of blood glucose (E) and the corresponding glucose AUC values (F). Means \pm SD, n = 6. ***P < 0.001 vs. saline.

In vivo toxicity of the impurity in **2c**.

After separating the deamidation byproduct (referred to as **impurity in 2c**), its *in vivo* toxicity was evaluated in Kunming mice and compared with that of **2c**.

Method

Acute toxicity assay of impurity in 2c

The toxicity test of **impurity in 2c** was conducted on Kunming mice for two weeks. Mice were randomly divided into three groups, and saline (control), **impurity in 2c** and **2c** ($1000 \text{ nmol}\cdot\text{kg}^{-1}$) were once daily *s.c.* injected for 14 days. Water and food were provided ad libitum during the experiment. At day 15, each group of mice were sacrificed and the whole blood were collected, and the blood samples were centrifuged to obtain serum. Blood urea nitrogen (BUN), alanine aminotransferase (ALT), serum creatinine (SCr), and aspartate aminotransferase (AST) were measured using biochemical analyzer (Beckman Coulter AU5811, Japan).

Results

As shown in Figure S2, compared with saline, no significant difference was observed for the key indexes of renal toxicity (SCr and BUN) and liver toxicity (AST and ALT) between **impurity in 2c** and **2c** treated groups, preliminary indicating the low toxicity of **impurity in 2c**.

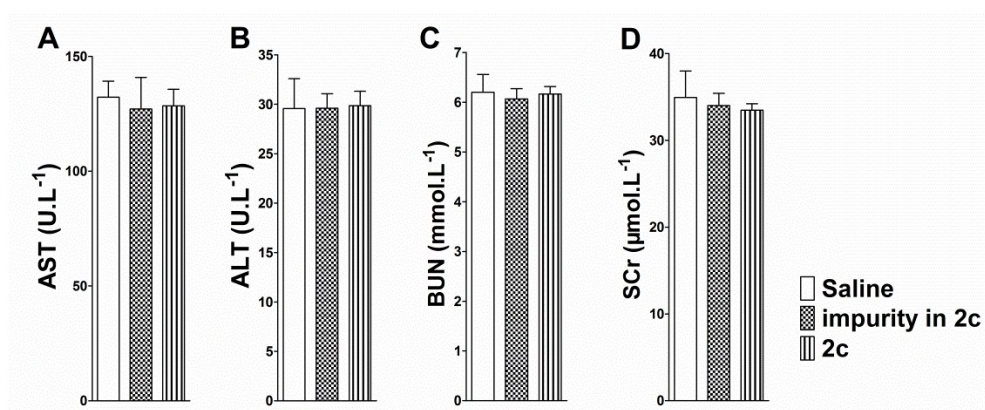


Figure S2. The acute toxicity assay of **impurity in 2c** and **2c** on Kunming mice. Saline (control), **impurity in 2c** and **2c** ($1000 \text{ nmol}\cdot\text{kg}^{-1}$) were once daily *s.c.* injected for 14 days. Biochemical analysis results of **impurity in 2c** and **2c** on AST (A), ALT (B), BUN (C) and SCr (D) after two weeks dosing on Kunming mice. Means \pm SD, $n = 6$.